

MODELING AND DESIGN OF KLYSTRON

Y. H. Chin

KEK, 1-1 Oho, Tsukuba-shi, Ibaraki-ken, 305, Japan

Abstract

We have developed a new method for a realistic and more accurate simulation of klystron using the MAGIC code. MAGIC is the 2.5-D or 3-D, fully electromagnetic and relativistic particle-in-cell code for self-consistent simulation of plasma. It solves the Maxwell equations in time domain at particle presence for a given geometrical structure. It uses no model or approximation for the beam-cavity interaction, and thus keeps all physical processes intact. With MAGIC, a comprehensive, full-scale simulation of klystron from cathode to collector can be carried out, unlike other codes that are specialized for simulation of only parts of klystron. It has been applied to the solenoid-focused KEK XB72K No.8 and No.9 klystrons, the SLAC XL-4 klystron, and the BINP PPM klystron. Simulation results for all of them show good agreements with measurements. We have also developed a systematic design method for high efficiency and low gradient traveling-wave (TW) output structure. All these inventions were crystallized in the design of a new solenoid-focused XB72K No.10. Its predicted performance is 126 MW output power (efficiency 48.5%) with peak surface field of about 77 MV/m, low enough to sustain a 1.5 μ s long pulse. It is now in manufacturing and testing is scheduled to start from November 1998.

1 JLC KLYSTRON PROGRAM

The 1-TeV JLC (Japan e^+e^- Linear Collider) project[1] requires about 3200 (linac) klystrons operating at 75 MW output power with 1.5 μ s pulse length. The main parameters of solenoid-focused klystron are tabulated in the second column of Table 1. The 120 MW-class X-band klystron program at KEK[2], originally designed for 80 MW peak power at 800 ns pulse length, has already produced 9 klystrons with solenoidal focusing system. To reduce the maximum surface field in the output cavity, the traveling-wave (TW) multi-cell structure has been adopted since the XB72K No.6. Four TW klystrons have been built and tested. All of them share the same gun (1.2 micropervance and the beam area convergence of 110:1) and the buncher (one input, two gain and one bunching cavities). Only the output structures have been redesigned each time at BINP. XB72K No.8 (5 cell TW) attained a power of 55 MW at 500 ns, but the efficiency is only 22%. XB72K No. 9 (4 cell TW) produced 72 MW at 520 kV for a short pulse of 200 ns so far. The efficiency is increased to 31% and no sign of RF instability has been observed. The limitation in the pulse length attributes a poor conditioning of the klystron. The latest tube, XB72K No.10, was designed at KEK, and is being build in Toshiba.

Apart from the solenoid-focused XB72K series, KEK has also started a PPM (periodic permanent magnet)

klystron development program. The design parameters are shown in the last column of Table 1. Its goal is to produce a 75MW PPM klystron with an efficiency of 60 % at 1.5 μ s or longer pulse. The first PPM klystron was designed and build by BINP in the collaboration with KEK. It has a gun with beam area convergence of 400:1 for the micropervance of 0.93. The PPM focusing system with 18 poles (9 periods) produces the constant peak magnetic field of 3.8 kG. The field in the output structure is still periodic, but tapered down to 2.4 kG. There are two solenoid coils located at the beam entrance for a smooth transport of a beam to the PPM section. It achieved 77 MW at 100 ns, but there is a clear sign of RF instability at higher frequencies. The DC current monitor in the collector shows about 30 % loss of particle when RF is on. The second PPM klystron, XB PPM No.1, is being designed at KEK.

Table 1: Specifications of X-band solenoid-focused and PPM-focused klystrons for JLC.

	XB72K	PPM
Operating frequency (GHz)	11.424	11.424
RF pulse length (μ s)	≥ 1.5	≥ 1.5
Peak output power (MW)	75	75
Repetition rate (pps)	120	120
RF efficiency (%)	47	60
Band-width (MHz)	100	120
Beam voltage (kV)	550	480
Perveance ($\times 10^{-6}$)	1.2	0.8
Maximum focusing field (kG)	6.5	
Gain (dB)	53-56	53-56

2 MAGIC CODE

After a series of disappointing performance of XB72K series, several lessons had been learned. First, KEK should have its own team to specialize the klystron design and overhaul the design process. Second, a new klystron simulation code was needed for a more realistic design of klystron, particularly, that of a TW output structure. The one-dimensional disk model code, DISKLY, had been used by BINP for design of the TW structure from XB72K No.5 till No.9. This code uses an equivalent circuit model (port approximation) to simulate a TW structure and tends to predict the efficiency much larger (nearly twice larger) than the experimental results. For the design of a new klystron, XB72K No.10, we have developed a method to use the MAGIC code[3] to simulate and design a klystron. MAGIC is the 2.5-D or 3-D, fully electromagnetic and relativistic particle-in-cell code for self-consistent

simulation of plasma. It solves the Maxwell equations directly at particle presence by the finite difference method in time like ABCI [4] or MAFIA. It requires only the geometrical structure of the cavity and assumes no model (neither port approximation nor equivalent circuit) for the beam-cavity interaction. The static magnetic field can be applied to a structure. Advantages of MAGIC are its accuracy and versatility. Even an electron gun can be simulated with results in good agreements with measurements. Simulation results can be imported/exported from one section of klystron to another, allowing a consistent simulation of the entire klystron without loss of physics. Only disadvantage is that it is time consuming.

3 FUNCTIONAL COMPARISON OF AVAILABLE CODES

Table 2 shows the functional comparison of computer codes available for klystron simulations. MAGIC is the only code that can simulate all parts of klystron from gun to collector. ARSENAL[5] is closest to MAGIC in functional performance, but cannot handle a TW multi-cell structure. CONDOR[6] can simulate a TW structure, but requires a beam input from a gun that needs to be simulated by other code such as EGUN[7]. In the migration of beam and fields from one code to another, two programs must be well matched to avoid any incomplete transfer of information and resulting unphysical phenomena.

Table 2: Functional comparison of available codes.

	Dimension	Gun	Buncher	Single-cell output cavity	Multi-cell output cavity
MAGIC	2.5, 3	○	○	○	○
EGUN	2.5	○	×	×	×
CONDOR	2.5	×	○	○	○
FCI [8]	2.5	×	○	○	×
ARSENAL	2.5	○	○	○	×
JPNDISK	1	×	○	○	×
DISKLY	1	×	○	○	×

4 SIMULATION METHOD USING MAGIC

We divide a klystron into three sections:

- Electron gun
- Buncher section (an input, gain and bunching cavities + drift space)
- TW output structure

The simulation techniques are described in detail in Ref. [9]. Here, we briefly summarize them.

3.1 Electron Gun

The gun simulation is done by specifying an emission area (cathode) and an applied voltage along a line between a wehnelt and an anode. The number of emitted particles can be specified per unit cell volume and unit time-step. The applied magnetic fields (both B_z and B_r) must be specified over the structure, not just on beam axis. They can be calculated using codes such as POISSON (for solenoid field) and PANDIRA[10] (for PPM). These programs requires the exact configuration of coils, yokes, or permanent magnets and their properties as input.

Figure 1 shows the comparison of beam profile simulated by EGUN and MAGIC for the XB72K-series gun. They look nearly identical. The simulated perveance for three different guns and the measured values are tabulated in Table 3. MAGIC simulations are in excellent agreement with the measurements, while the EGUN tends to produce a 5-10 % larger value than the measurements. This behavior was also reported in simulation of SLAC 50 MW PPM klystron by EGUN [11].

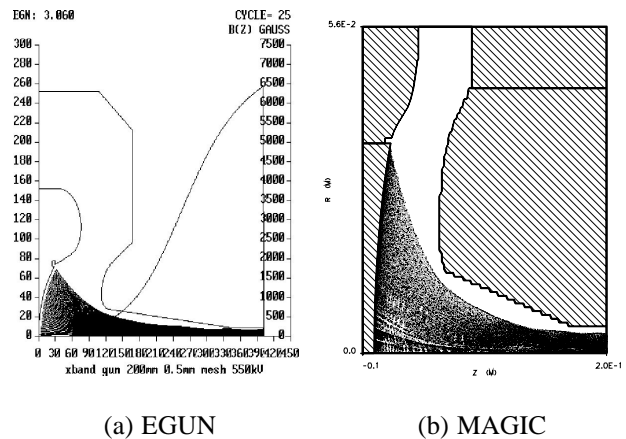


Figure 1: Beam profile from the XB72K gun simulated by (a) EGUN and (b) MAGIC.

Table 3: Comparison of the simulated perveances and the measured values.

Klystron	Frequency (MHz)	Micro perveance		
		MAGIC	EGUN	Measured
XB 72K (KEK)	11,424	2.03	1.89	2.05
PV3030 (KEK)	2,856	1.19	1.10	1.2
5045 (SLAC)	2,856	1.99	1.78	2.0

3.2 Buncher Section

The input cavity needs a different treatment from other cavities, because the RF power is given externally, rather than being induced by a beam. Since a beam stays almost

as DC while passing the input cavity, the beam induced voltage is negligible. Therefore, we just need to specify the applied RF voltage along an electric field line between the cavity gap. The field distribution of the fundamental mode should be computed by MAGIC priority and used as input. Other cavities need to be tuned to correct fundamental frequencies by adjusting the cavity aperture on mesh. The beam-induced voltage in cavities are monitored to measure the necessary RF cycles for saturation. In most of cases, about 200-300 RF cycles are enough. To speed up the saturation, a DC beam current from gun is increased smoothly and slowly from zero to the full value at the first 10-20 RF cycles.

Figures 2 (a) and (b) show spatial distributions of beam in the input+gain cavity section and in the bunching cavity section of the XB72K No.10 buncher, respectively. The strong bunching of beam (RF current/DC current ≈ 1.7) is created toward the end of the buncher section.

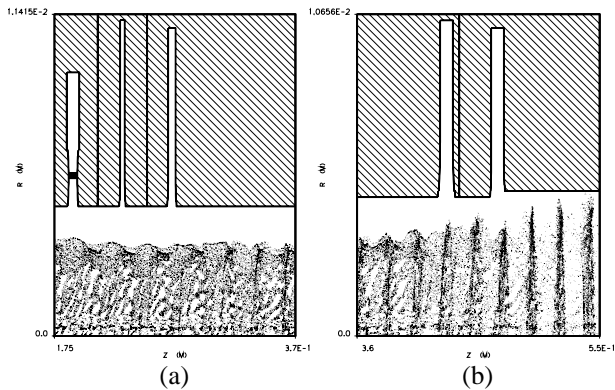


Figure 2: Spatial distribution of beam (a) in the input+gain cavity section and (b) in the bunching cavity section of the XB72K No.10 buncher.

3.3 Traveling-Wave (TW) Output Structure

Simulation of TW output structure is quite straightforward as any other cavity. In order to simulate effects of a non-axis-symmetrical output coupler by the 2.5-D version of MAGIC, we model it by a ring-shaped conductor which has the same complex S_{11} -matrix element (i.e., the reflection coefficient for amplitude and phase). This is illustrated in Fig. 3. There are three free parameters to fit the frequency dependent S_{11} -matrix element: the conductance, and the inner and the outer radii of the conductor. For details of the output coupler modeling, refer to Ref.[9]. As shown later, simulation results for many klystrons seem to verify the validity of this approximation.

Before inventing the above conductor approximation, we have considered a use of an axis-symmetrical radial transmission line to model a 3-D coupler. However, this method cuts the output structure into two disconnected parts, and thus an artificial DC voltage is induced by the DC component of beam at the output cell to which the output couplers are attached. This artificial DC voltage causes a non-negligible effect to the particle dynamics,

and results in error. Figure 4 shows the simulation results for the output structure of XB72K No.10.

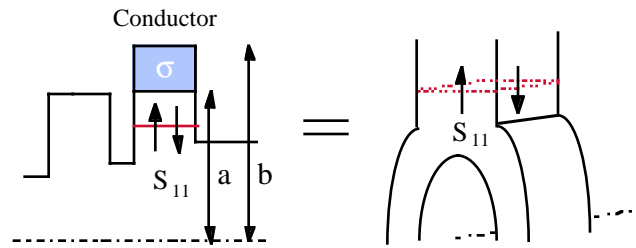


Figure 3: Illustration for 2.5-D modeling of 3-D output coupler using a conductor.

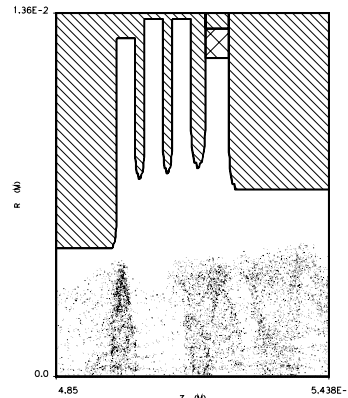


Figure 4: Simulation of XB72K No. 10 in the output structure.

5 SIMULATION RESULTS AND MEASUREMENTS

Figure 5 shows the simulation results of MAGIC and the experimental data for the saturated output power vs. beam voltage for XB72K No.8 klystron. Excellent agreements can be seen. The closed triangles in Fig. 5 are DISKLY simulations. It reveals the accuracy limitation of the 1-D disk model code.

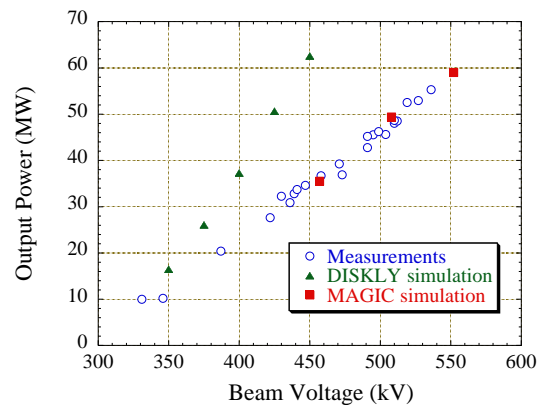


Figure 5: Simulation results of MAGIC and DISKLY and the measurement data for XB72K No.8 klystron.

Let us move to the simulation of SLAC XL-4 klystron. XL-4 klystron produced 50 MW at 400 kV with

1.5 μs pulses at 120 pps. It attained 75MW at 450 kV, but the pulse length could go up only to 1.2 μs before the RF breakdown in the output cavity. The simulation results for the output power are compared with the measurements in Fig. 6. MAGIC simulations reproduce the measurement data quite well. The CONDOR prediction at 450 kV, denoted by the closed triangle, was at 10% too high. Figure 7 shows the output power vs. the input power for XL-4. It is clear that the simulation reproduces the measured gain curve well.

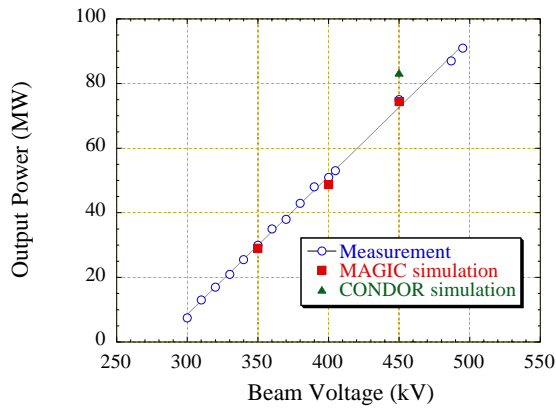


Figure 6: Simulation results of MAGIC and CONDOR and the measurement data for the SLAC XL-4 klystron.

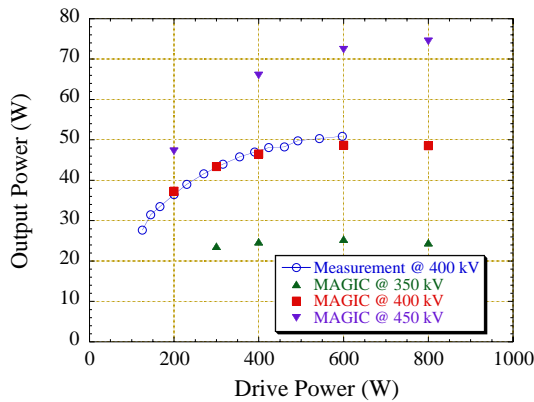


Figure 7: Simulations and measurement data of the output power vs. the input power for the SLAC XL-4 klystron.

Our simulation method can also make an accurate prediction of performance for a PPM klystron. Figure 8 shows the simulation results and the measured values of output power for the BINP PPM klystron. The evolution of DC and RF beam current as a function of distance from the gun is plotted in Fig. 9. The sudden drop of the DC current is due to the particle interception at the final cell of the output cavity. The interception is caused by lack of focusing for particles that drop to the stop-band voltage after losing energy to the traveling-wave. This simulation result explains the experimental observation of significant particle loss described in Section 1.

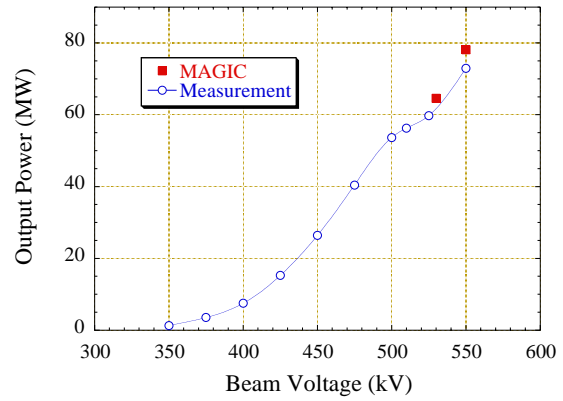


Figure 8: Simulation results for the BINP PPM klystron.

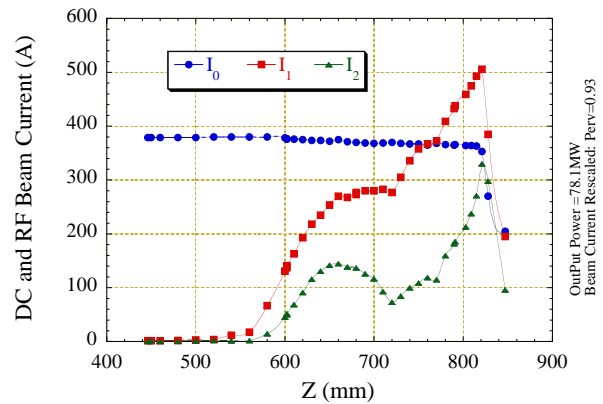


Figure 9: Evolution of the DC and RF beam current in the BINP PPM klystron.

3 XB72K NO.10 DESIGN

XB72K No.10 is the last solenoid-focused klystron in the XB72K series. Main changes from the previous XB72K klystrons are the buncher section and the TW output structure. The operational experience with the previous klystrons proved that the gun portion of XB72K has sufficient performance (1.2 micropervance at 2 μs pulse length) and no interception of particles has been observed. The old buncher has two gain cavities and only one bunching cavity. It has a poor RF power generation capability: the RF current /DC current is only 1.2 at the entrance of the output structure. In XB72K No.10, one more bunching cavity was added and the drift space was lengthened to 16cm. The stagger tuning of gain cavities was also adopted to increase the band-width to the current specification of 100 MHz.

The most challenging part of XB72K No. 10 design is a high efficiency and low gradient TW output structure. MAGIC is quite useful for getting an accurate estimate of klystron performance, but the design of an effective TW structure is another matter. A systematic design method was needed to avoid getting lost in the freedom of too many parameters.

For this end, we have developed a simple-minded theory of a constant group/phase velocity TW structure. The idea

is to let the power flow with a constant group velocity throughout the structure, while evolving due to merge of the extracted power from a beam. The Q-value at the output port is matched to this group velocity so that the power exits at the same speed as it flows in the structure. This smooth flow of power prevents congestion at local spots and thus the electromagnetic energy density is more equally distributed in the structure

It is also better to keep the phase velocity constant (approximately equal to the average beam velocity) from the first to the last cell, rather than being matched with the declining beam velocity. When the perfect synchronization of traveling-wave and the beam is tried, the beam loses energy too quickly to the wave, and its velocity becomes too slow to be matched with the wave after a few cells (XB72K No. 10 has four cells). The beam then moves to the acceleration phase of the wave and starts to get energy back. The energy extraction efficiency of each cell does not have to be too good. Only the total efficiency of all cells matters. It is more important to keep the beam in the deceleration phase of the wave all the time. In our method, the traveling-wave travels behind the beam at first, and catches it up with in the middle of the structure. It then moves ahead of the beam, but exits from the output port before the beam slips into the acceleration phase of the wave.

We also demand that each cell is operated in $2/3\pi$ mode at 11.424 GHz. The cell length is also constant except the last cell (slightly longer to reduce the field gradient). As the result, the cells become almost identical. We then tapered up the iris aperture slightly to equalize the field gradient among the cells. In this method, once the group and the phase velocities are chosen, the geometry of the structure are almost uniquely determined. The structure of output port can be adjusted to control the reflection of power to maximize the output power.

The predicted output power vs. the beam voltage is plotted in Fig. 10:

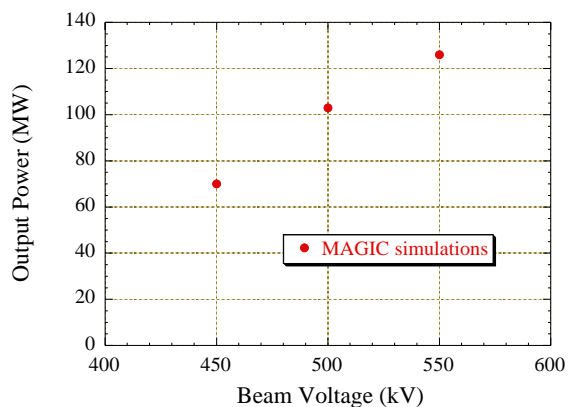


Figure 10: Predicted output power vs. beam voltage for the XB72K No.10.

The predicted performance is summarized in Table 4. Figure 11 shows comparison between XB72K No.10 and

SLAC XL-4 for the saturated power vs. the maximum field gradient in the output structure. Both have similar efficiencies of about 48%, but the maximum gradient of XB72K No.10 is about 20% lower than that of XL-4, though the power is 67% larger. In XB72K No.10, the fairly constant gradient is achieved in the output structure. This comparison indicates that the XB72K TW output structure can attain 120 MW power at a longer pulse than XL-4 at 75 MW without cavity breakdown. At 75MW, XB72K can tolerate an even longer pulse. It is now in manufacturing and testing will begin in November 1998.

Table 4: Predicted performance of XB72K No. 10.

Peak output power	126 MW
Beam voltage	550 kV
Efficiency	48.5%
Maximum field gradient in TW	77 MV/m
Pulse length	1.5 μ s or longer
Band-width	100 MHz
Gain	53 dB

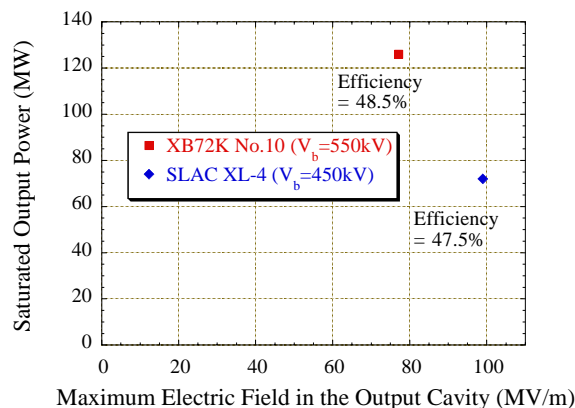


Figure 11: Saturated power versus the maximum field gradient in the output structure for XB72K No.10 and SLAC XL-4.

REFERENCES

- [1] JLC Design Study, KEK, April 1997.
- [2] Y. H. Chin, et. al., in Proc. of EPAC98, 1998.
- [3] MAGIC User's Manual, Mission Research Corporation, MRC/WDC-R-409, 1997.
- [4] Y. H. Chin, "User's Guide for ABCI Version 8.8", LBL-35258 and CERN SL/94-02 (AP (1994)).
- [5] A. N. Sandalov, et. al., in Prof. of RF96, KEK Proc. 97-1, pp.185-194, 1997.
- [6] B. Aimonetti, et. al., "CONDOR User's Guide", Livermore Computing Systems Document, 1988.
- [7] W. B. Herrmannsfeldt, SLAC-PUB-6498 (1994).
- [8] T. Shintake, Nucl. Instr. Methods A363, p.83, 1995.
- [9] S. Michizono, S. Matsumoto, and H. Tsutsui in this proceedings.
- [10] J. Billen and L. M. Young, "POISSON SUPERFISH", LA-UR-96-1834 (1997).
- [11] D. Sprehn et.al, in Proc. of RF96, KEK Proc. 97-1. pp.81-90, 1997.